INFLUENCE OF DEFLECTION HOLE ANGLE ON EFFUSION COOLING IN A REAL COMBUSTION CHAMBER CONDITION

by

Xiao LIU* and Hongtao ZHENG

College of Power and Energy Engineering, Harbin Engineering University, Harbin, China

Original scientific paper
DOI: 10.2298/TSCI140107043L

Fluid-solid coupling simulation is conducted to investigate the performance of effusion cooling in the real combustion chamber condition of strong rotation and primary holes. The wall temperature and film cooling effectiveness of different deflection angle is analyzed. From the results, it is concluded that the performance of effusion is better than conventional film cooling. The wall temperature and gradient is lower, the cooling efficiency is higher and the coolant is reduced by 20%, but pressure loss is slightly increased. The cooling effectiveness decreases behind primary holes because of local combustion. Comparison with the effect of deflection angle, the cooling performance of 60 deg deflection angle is best. The coolant is better attached to the wall downstream when the deflection angle is same as the rotating mainstream. In addition, the effect of deflection angle is not so significant on the coolant flow rate, but a large negative impact on the pressure loss. Although the cooling effectiveness of 60 deg deflection angle is highest, the total pressure recovery coefficient is lower. The maximum temperature drops about 70 K and the outlet temperature distribution trends more consistent. So various factors should be taken into consideration when designing of deflection angle.

Key words: *combustor, effusion cooling, deflection angle, cooling effectiveness, CFD simulation*

Introduction

High temperature rise of combustion chamber is required for the development of modern aero-engines. This trend results in coolant flow rate reduction used for protecting combustor liner wall, so the requirement of combustion and cooling air forms a contradiction. There is an urgent need to adopt high temperature resistant alloy material or an efficient combustor liner cooling technology. As the development pace of high-temperature materials cannot meet the needs of aviation engine technology, so the cooling technology is playing an increasingly significant role in advanced aero-engines.

Today four main cooling systems are implemented to preserve the liner performance: general film cooling, transpiration, effusion and impingement cooling [1], and the importance of the cooling has been given more attention. Li *et al*. [2] conducted investigations to understand the characteristics of the flow, combustion, cooling performance and their interaction in an aero-engine combustor by fluid-solid coupling simulation. Ali *et al*. [3] elucidated the effective-

* Corresponding author; e-mail: liuxiao_heu@163.com

ness of a cooling system in the protection of combustor walls by numerical simulations in a gas turbine swirl stabilized combustor. Yu *et al.* [4] presented the relationship between the angles of the hole, the orientations of the flow injection and the film-cooling effectiveness in the transition piece of combustor. The effusion cooling is regarded as one between the general film and transpiration cooling technology, and an effusion cooling system consists of three cooling processes: convection cooling on cold-side, the cooling effect inside the inclined holes and film cooling on hot-side wall surface. Both numerical and experimental investigations on effusion film cooling have been conducted by many researchers. Andrews *et al.* [5-7] studied the influence of cooling hole size, pitch, and inclination angle through a number of experiments. Experimental and numerical investigations were performed on the overall cooling effectiveness by Lin [8-10]. The test plates had different hole-spacing, different deflection angle, and different inclination angle, and it was mainly focused on studying the influence of hole geometrical parameters and blowing ratio on film cooling. Scrittore *et al*. [11,12] measured velocity profiles and dilution hole injection effect on effusion behavior. They found that blowing ratios had a very low effect of blowing ratio on cooling performance, the dilution hole injection leaded to an increased spreading of coolant jets. Goldstein [13] studied the film cooling performance downstream of one row of holes with 35 deg inclination angle, 45 deg compound angle, and 3*d* hole spacing. Ling *et al*. [14] obtained the film cooling effectiveness and heat transfer coefficient in a full coverage film cooling wall with different hole-spacing of 16*d* to 10*d*, using the transient liquid crystal technique. Gustafsson *et al.* [15] investigated the temperature distribution on effusion-cooled plates with different parameters of temperature ratios, velocity ratios, injection hole-spacing, inclination angle, and thermal conductivity of the test plates. Yang *et al*. [16] investigated the evolution of the film by many multi-hole arrangements at several blowing ratios. Harrington *et al.* [17] studied the effect of the mainstream turbulence on the adiabatic effectiveness of large-scaled full coverage film cooling plates. Facchini *et al*. [18] investigated the influence of a re-circulation area in the mainstream. They obtained that the presence of the re-circulation leaded to a general reduction of effectiveness.

From the open literatures of effusion cooling, it is found that most of the research results were obtained from the simplified model (flat plate, uniform hot mainstream and coolant air). There are big differences in the cooling structure and air-inlet condition between the model and real combustion chamber, which will have a huge impact on the flow and heat transfer characteristics: (1) the big holes (primary and dilution hole) exist in the combustion chamber and (2) there is a strong tangential velocity with the effect of swirler. But it generally ignored those effects in the simplified model. So the current work employed fluid-solid coupling simulation by FLUENT 12.0 to study the wall temperature and film cooling effectiveness of different deflection angle on the real combustion chamber condition.

Model description

The governing equations are solved using CFD package ANSYS FLUENT 12.0. The SIMPLE method was used for velocity-pressure coupling. A second-order discretization scheme was used to solve all governing equations. This paper adopted Euler method to calculate gas flow and Lagrange method to calculate discrete phase, when using Lagrange method, time particle residence time will be solved. In addition, realizable k-ε model, probability density function (PDF) combustion model and radiation model were used to calculate chemical reaction with turbulence.

Turbulence model

As the simplest "complete models" to predict the turbulent combustion reaction, the realizable model is widely used in swirl turbulent combustion in the past few years [19, 20], it has been extensively validated for a wide range of flows. The fundamental equations of realizable k-ε model are:

$$\frac{\partial(\rho k)}{\partial t} + \nabla(\rho\vec{\mathrm{V}}k) = \nabla(\Gamma_{\mathrm{k}}\nabla k) + G_{\mathrm{k}} + G_{\mathrm{b}} - \rho\varepsilon - Y_{\mathrm{k}} + S_{\mathrm{k}} \tag{1}$$

$$\frac{\partial(\rho\varepsilon)}{\partial t} + \nabla(\rho\vec{\mathrm{V}}\varepsilon) = \nabla(\Gamma_{\varepsilon}\nabla\varepsilon) + \rho C_1 S\varepsilon - \rho C_2 \frac{\varepsilon^2}{k+\sqrt{\nu\varepsilon}} + C_{1\varepsilon}\frac{\varepsilon}{k}C_{3\varepsilon}G_b + S_{\varepsilon} \tag{2}$$

Combustion model

The hydrocarbon fuel's burning is extremely complex, it is impossible to describe combustion performance with one particular combustion model, so it is needed to simplify combustion characteristic. At the basic of simple chemical reaction system hypothesis, we ignored chemical reaction mechanism to calculate combustion flow field. The major researched object is average-thermal-effect. The fast chemical reaction model which based on simple probability density function (PDF) has been used to simulate fuel oil burning. To close combustion modeling, β function was adopted to describe turbulence fluctuation instantaneous characteristic of conservation variable mix fraction. The complete chemical reaction equation is:

$$\mathrm{C_{12}H_{23}} + 35.5\mathrm{O_2} \rightarrow 12\mathrm{CO_2} + 11.5\mathrm{H_2O} \tag{3}$$

Under the assumption of equal diffusivities, the species equations can be reduced to a single equation for the mixture fraction, f. The reaction source terms in the species equations cancel (since elements are conserved in chemical reactions), and thus f is a conserved quantity. While the assumption of equal diffusivities is problematic for laminar flows, it is generally acceptable for turbulent flows where turbulent convection overwhelms molecular diffusion. The Favre mean (density-averaged) mixture fraction equation is:

$$\frac{\partial}{\partial t}(\rho\bar{f}) + \nabla(\rho\vec{\mathrm{v}}\bar{f}) = \nabla\left(\frac{\mu_{\mathrm{t}}}{\sigma_{\mathrm{t}}}\nabla\bar{f}\right) + S_{\mathrm{m}} + S_{\mathrm{user}} \tag{4}$$

The source term S_{m} is due solely to transfer of mass into the gas phase from liquid fuel droplets or reacting particles. S_{user} is any user-defined source term.

In addition to solving for the Favre mean mixture fraction, ANSYS FLUENT solves a conservation equation for the mixture fraction variance, $\overline{f'^2}$:

$$\frac{\partial}{\partial t}(\rho\overline{f'^2}) + \nabla(\rho\vec{\mathrm{v}}\overline{f'^2}) = \nabla\left(\frac{\mu_{\mathrm{t}}}{\sigma_{\mathrm{t}}}\nabla\overline{f'^2}\right) + C_{\mathrm{g}}\mu_{\mathrm{t}}(\nabla\bar{f})^2 - C_{\mathrm{d}}\rho\frac{\varepsilon}{k}\overline{f'^2} + S_{\mathrm{user}} \tag{5}$$

where $f' = f - \bar{f}$. The default values for the constants σ_{t}, C_{g}, and C_{d} are 0.85, 2.86, and 2.0, respectively, and S_{user} is any user-defined source term.

The probability density function, written as $p(f)$, can be thought of as the fraction of time that the fluid spends in the vicinity of the state f. The fluctuating value of f, spends some fraction of time in the range denoted as Δf·$p(f)$, takes on values such that the area under its curve in the band denoted, Δf, is equal to the fraction of time that f spends in this range. Written mathematically:

$$p(f)\Delta f = \lim_{T\to\infty}\frac{1}{T}\sum_i \tau_i \tag{6}$$

where T is the time scale and τ_i – the amount of time that t spends in the Δf band. The shape of the function $p(f)$ depends on the nature of the turbulent fluctuations in f. In practice, $p(f)$ is unknown and is modeled as a mathematical function that approximates the actual PDF shapes that have been observed experimentally.

The probability density function $p(f)$, describing the temporal fluctuations of f in the turbulent flow, can be used to compute averaged values of variables that depend on f. Density-weighted mean species mass fractions and temperature can be computed as

$$\bar{\phi}_i = \int_0^1 p(f)\phi_i(f)\mathrm{d}f \tag{7}$$

Importantly, the PDF shape $p(f)$ is a function of only its first two moments, namely the mean mixture fraction, f, and the mixture fraction variance, f'^2. Thus, given ANSYS FLUENT's prediction of f and f'^2 at each point in the flow field (eqs. 4 and 5), the assumed PDF shape can be computed and used as the weighting function to determine the mean values of species mass fractions, density, and temperature.

Radiation model

The discrete ordinate radiation model [21] was used in this work, as it is applicable across a wide range of optical thicknesses. The model solves the radiative transfer equation (RTE) for a finite number of discrete solid angles across the computational domain. It also incorporates the weighted sum of gray gas model (WSGG), in which spatial variation in the total emissivity is computed as a function of gas composition and temperature. The WSGG is a reasonable compromise between the oversimplified gray gas model and a complete model, which takes into account particular absorption bands.

Results and discussion

Meshing and model validation

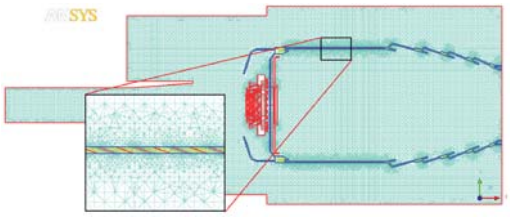

Figure 1. 2-D view of cross-section for combustor with effusion cooling

Unstructured tetrahedral meshes were used for simulation computation by ANSYS ICEM CFD. The total mesh number of general film cooling model is 7.0e+06 after grid independence analysis. Due to refining of multi small holes, the mesh number increases to 1.0e+07. Figure 1 shows the tetrahedral meshes of 2-D view of cross-section for combustor with effusion cooling. It can be seen that, near the cooling holes, the grid is refined, there are at least 10 nodes at each hole for accurate simulation.

In this paper, the experimental data [22] of an annular combustion chamber was used for model validation. The infrared imaging technique was used for the non-intrusive surface temperature measurements. Cold (air mass flow 0.24 kg/s, 500 K) and three gas oil ratio (f = 0.01950, 0.02600, 0.03308) combustion fields were calculated and compared. The fuel temperature is 300 K and operating pressure is 0.13 MPa. Experiment system and the double swirl annular combustor geometry (1/24) was shown in fig. 2, the detailed description can be found in [22].

Figure 2. Experiment system and the double swirl annular combustor geometry

Under the experimental conditions, the combustion flame considered is a turbulent diffusion flame. Figure 3 shows the streamlines of particle image velocimetry (PIV) experiment and different turbulence model. A counter-rotating vortex pair (CRVP) can be easily seen, which ensures the ignition and flame stability formed in the head zone of the combustor. The predicted streamlines obtained by k-ε model are in good agreement with PIV. Vortex pitch is so accurate, shoving that simulation of strong rotational flow is pretty well.

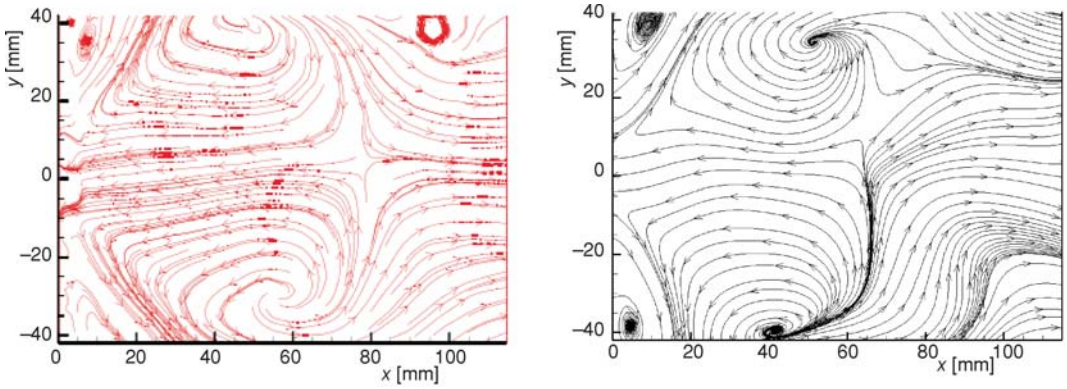

Figure 3. Streamline of PIV experiment and realizable k-ε model prediction

Figure 4 shows the profiles of temperature on radial outlet at different gas-oil ratio. It also shows a very good agreement with the experimental data, which reveals that the general trend of temperature and combustion products can be predicted correctly by the realizable k-ε model and PDF combustion.

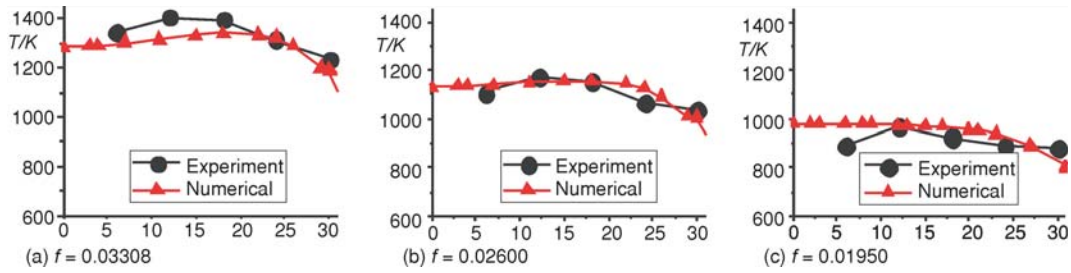

Figure 4. Profiles of combustor outlet temperature on radial

The prototype combustor liner is cooled by the full film from discrete tiny holes with the average diameter 2 mm. The temperature dependences of the thermal conductivity (λ_s) and the specific heat capacity (C_s) of the solid material were incorporated using polynomial functions, shown in formula (8) and (9):

$$\lambda_s = 9.946 + 0.018T - 1.489 \cdot 10^{-5} T^2 + 1.364 \cdot 10^{-8} T^3 \tag{8}$$

$$C_s = 411.222 + 0.293T - 2.412 \cdot 10^{-4} T^2 + 1.507 \cdot 10^{-7} T^3 \tag{9}$$

The wall temperature was performed using the infrared (IR) imaging technique and the experimental and simulated temperature contour of general film cooling is show in fig. 5. It is observed that the temperature distribution and trend of simulation are in good agreement with the measured ones. High temperature zone appears behind the primary holes, the reason of this phenomenon is because that any strong injection may penetrate and damage the film. In addition, the air from primary hole is almost perpendicular to the mainstream, and a re-circulation zone exists, so the fuel is burning close to the flame tube wall. To aid better comparisons with different effusion patterns, there are two lines along the middle section (line 1) and the center of primary and dilution holes (line 2) to study the trend of combustor liner temperature and cooling efficiency.

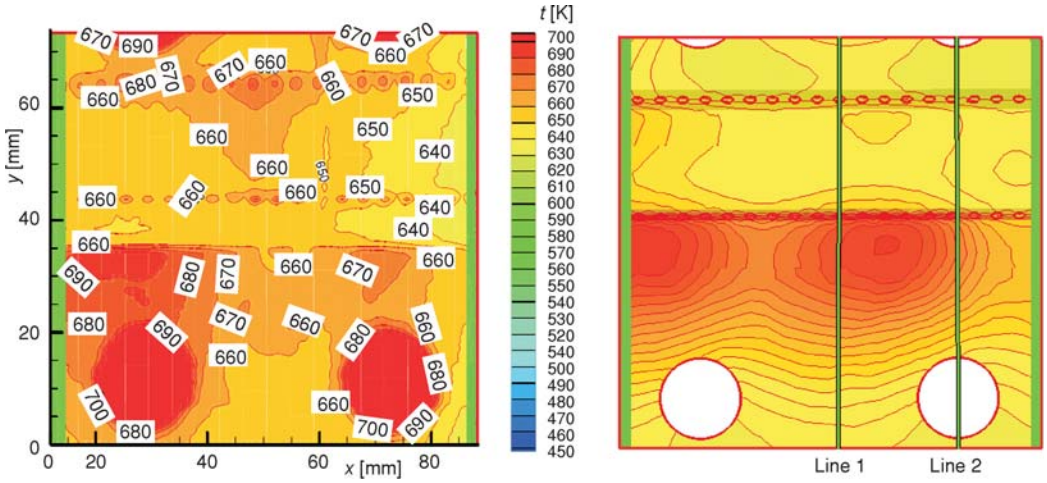

Figure 5. Experimental and simulated temperature contour

Analysis of cooling effect

In general, for effusion cooling, the diameter d is 0.3-0.7 mm, the spanwise direction ratio P/d is 2-10, the streamwise direction ratio S/d is 2-10, the inclined angle is 20-120 deg [17]. In this paper, the general film cooling with diameter 2 mm was changed into the staggered effusion cooling in the front of flame tube. Figure 6 illustrates this cooling structure. Setting that when the deflection angle is same as the direction of swirler rotation, the angle is positive. The size of the inclined effusion cooling wall is 110 × 100 mm (length × width), and the thickness of wall is $\delta = 2$ mm. The diameter of effusion hole is $d = 0.7$ mm, $P/d = 8$, $S/d = 5$, staggered spacing $H = 0.5P$. Every effusion hole has an inclined angle of $\alpha = 30$ deg with respect to the surface and the deflection angle of effusion hole is set to be 0, 30, 60, and –60 deg, respectively.

Figure 7 shows the temperature distribution of different deflection angles, respectively. For general film cooling, the cold air from film cooling hole will form a film layer to protect the wall on hot-side. The temperature near downstream of the cooling hole is low, however, the cooling capacity declines with the increase of distance. There is a local high temperature zone behind the primary hole and it will reduce the service life of the flame tube. For the effusion cooling, the temperature distribution becomes more uniform. The cooling performance of 60 deg is better than others and the –60 deg is the worst. There is a large temperature gradient behind the primary holes along the axial direction for 0 and –60 deg, but it is still better than the effect of general film cooling, which means the good cooling performance of combustor liner using effusion cooling technology.

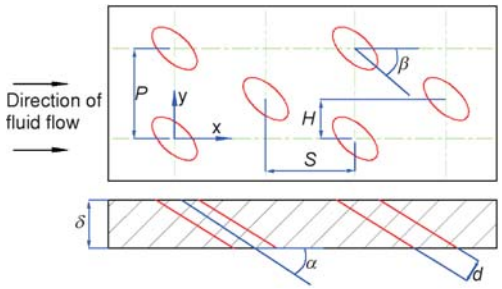

Figure 6. Structure of effusion cooling

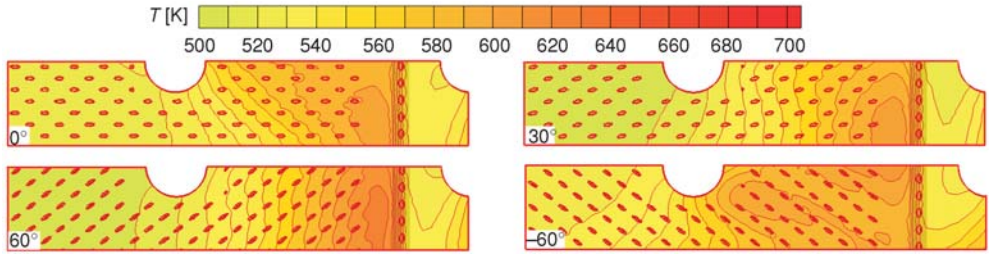

Figure 7. Temperature distribution of different deflection angles

In addition, the trends of temperature along two lines are shown in fig. 8. It is easily seen that the temperature at the starting of the wall is low as air inlet, then it starts to rise rapidly after the primary hole. The 60 deg hole angle model has the best effect, only consider the wall temperature distribution. According to the conclusion of Gustafsson *et al.* [15], the arrangement of the holes should be more dense to protect the behind primary holes where is the easiest section of high temperature.

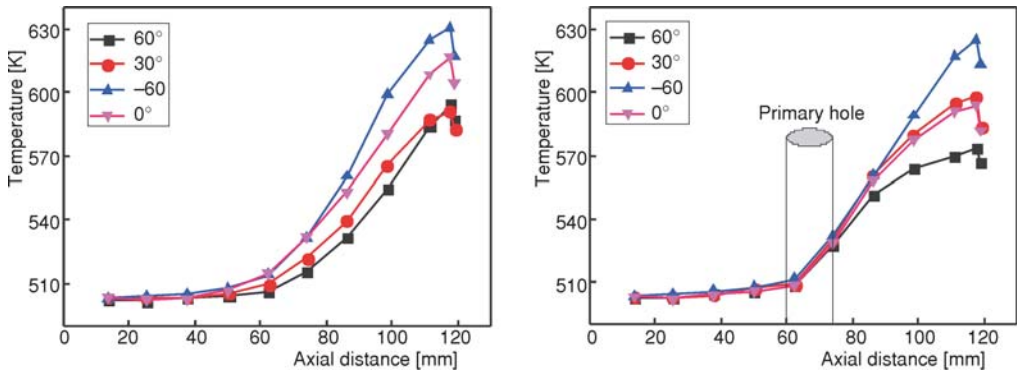

Figure 8. Temperature along two lines

Figure 9 shows the velocity vector diagram of cooling air from one of effusion holes, which locates at the middle row. The middle part of diagram is velocity vector from internal effusion cooling hole, the upper part is the cooling air in the channel and the lower part is the film flow near the flame tube. The flow behavior after each row of the film cooling holes varies a lot because of geometry. The velocity of 0 deg is highest and the –60 deg is lowest. In addition, the mainstream direction is clockwise due to the swirler, so the flow from cooling holes deflects a little to the right. When the velocity is low, the cooling airflow is close to the wall and the deflection angle is same as the rotating mainstream, the coolant is well attached to the surface downstream.

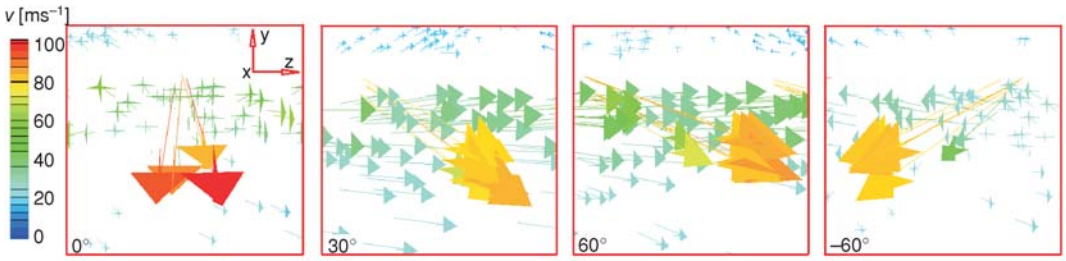

Figure 9. Velocity vector diagram of cooling air

Total pressure recovery coefficient is generally used to characterize the performance of the combustion chamber, which is defined as the following formula:

$$\sigma_B = \frac{P_{t4}}{P_{t3}}$$

where, P_{t3} and P_{t4} mean the average total pressure in import and export section of combustion chamber, respectively.

The flow rate of cooling air in prototype combustor liner is 29% and the reconstructive part (RP) is 4.95% as shown in fig. 10(a). The flow rate of effusion cooling is about 20% lower than general film cooling. This is because the flow area of inclined holes increases and the direction of angle is the same as mainstream causing by swirler. That means the combustion air becomes more, which will meet the high temperature rise of combustion chamber for the development of modern aero-engines. However, the influence of different angle is not so significant.

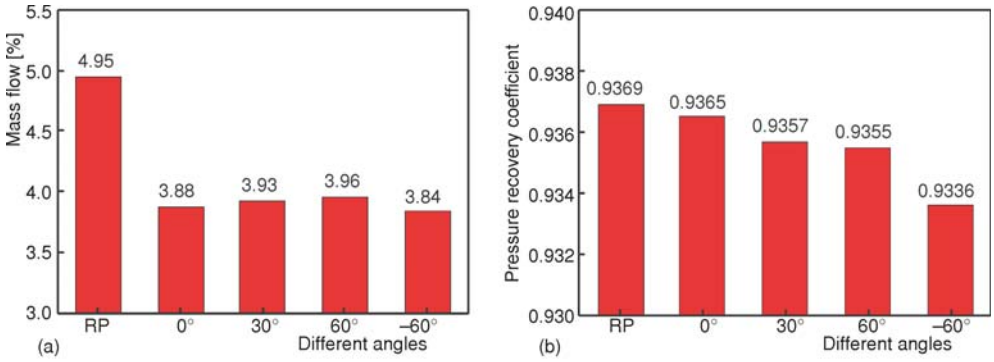

Figure 10. Flow rate of cooling air and total pressure recovery coefficient

Another important factor is total pressure recovery coefficient. The lower coefficient is, the gas turbine power losses, the fuel consumption rate is higher. The coefficient of prototype combustor is 93.69% as shown in fig. 10(b), and the reconstructive combustor is lower to 93.36% because of the longer cooling holes, so the friction loss of boundary layer increases. Although the cooling performance of 60 deg is best, the total pressure recovery coefficient is lower.

The cooling effectiveness (η) is used to characterize the performance of film cooling. The η is defined as:

$$\eta = \frac{T_m - T_{aw}}{T_m - T_c} \tag{10}$$

where T_m is the combustion gas temperature near combustor liner. T_c and T_{aw} are the temperature of the coolant and the temperature of the wall, respectively.

In fig. 11, comparison of cooling effectiveness of four hole angles is shown along the axial direction. The curve of effectiveness of line 1 forms a M shape. The effectiveness at the beginning of the film is low, since the film is still not fully development and the combustion in the tube head zone is not sufficient. Then, the cooling effectiveness rises and reaches maximum when axis locates at 60 mm, just before the primary holes, and keeps at the high value. At the end of test wall, it goes down rapidly because that there is no cooling holes and the cooling of wall just depends on the film developed from upstream. For line 2, there is only one different change behind the primary holes, the cooling effectiveness declines because the film is damaged by the strong injection, moreover, local combustion also occurs here close to the flame tube wall. Compared with different angles, the cooling effectiveness of the 60 deg achieves higher, which can protect the inner surface well. Therefore, taking all the factors into consideration, the cooling performance of 60 deg is best: internal heat convection of hole is enhanced due to the large length-diameter ratio, which can increase the internal surface area available for heat removal; the coolant discharged from the holes forms a cooling film, which is well attached to the surfaces downstream because of the same direction with mainstream.

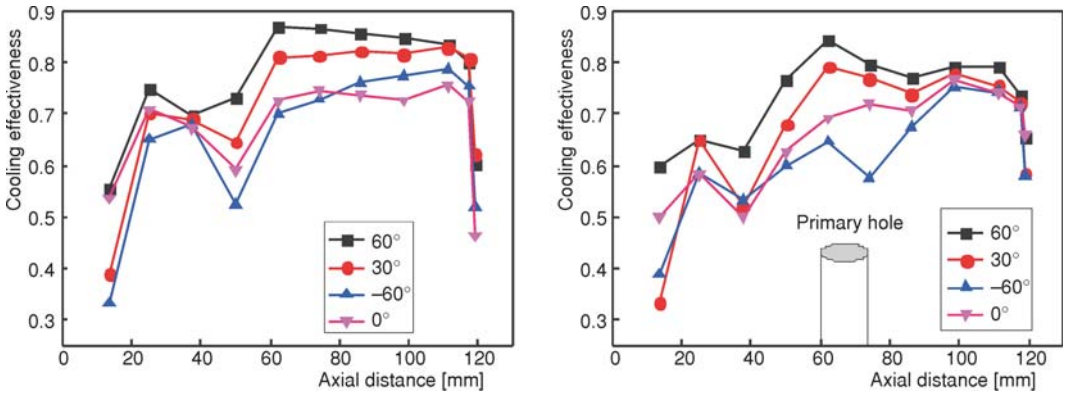

Figure 11. Cooling effectiveness along two lines (line 1 – left figure, line 2 – right figure)

Analysis of temperature distribution

Since the different angle of inclination has little effect on combustion field according to the simulation, it only shows the temperature distribution in middle section and outlet of general film cooling and effusion cooling with 60 deg angle of inclination, in figs. 12 and 13.

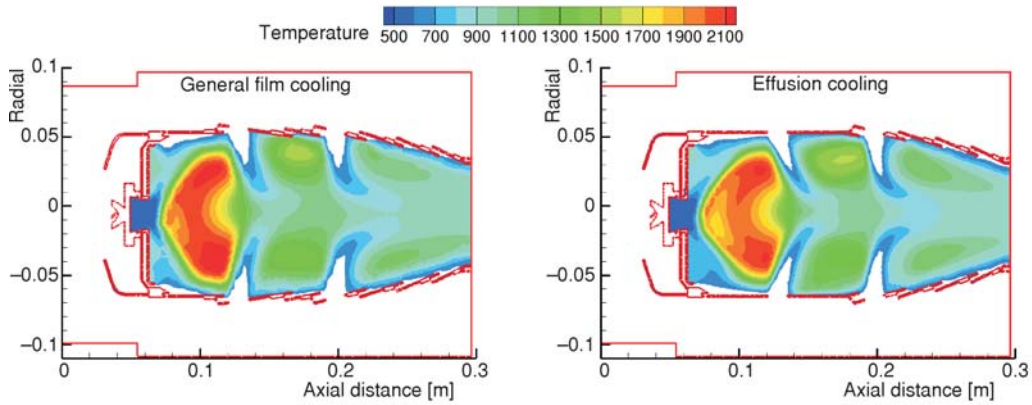

Figure 12. Temperature distribution in middle section

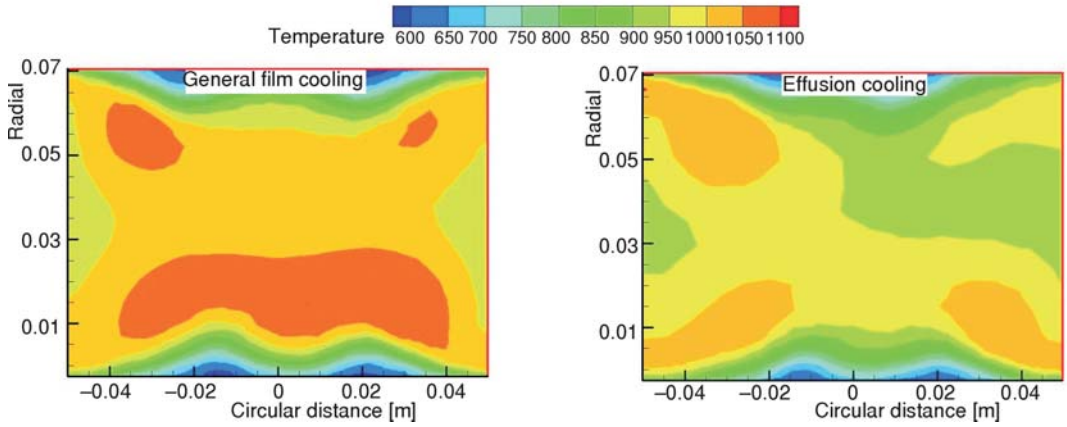

Figure 13. Temperature distribution at outlet

According to the principle of combustion energy conservation, the combustion efficiency is defined as the ratio of the difference enthalpy of import and export and the fuel enthalpy:

$$\eta_{\mathrm{r}} = \frac{G_{\mathrm{g}} C_{pg} (T_{\mathrm{g}}^{*} - T_0) - G_{\mathrm{a}} C_{\mathrm{pa}} (T_{\mathrm{a}}^{*} - T_0) - G_{\mathrm{f}} C_{pg} (T_{\mathrm{f}}^{*} - T_0)}{G_{\mathrm{f}} Q_H^f}$$

where G means mass flow rate, C_p – the means specific heat, g – the means gas, a – the means air, f – the means fuel, and Q_H^f [J/kg] – means the low heat value under the reference temperature (293 K).

Due to the amount of cooling air reduces, which will increase the air flow rate from the swirler, the primary and dilution holes. The main combustion zone moves backward slightly, the depth of the air jet increases. The maximum temperature drops about 70 K, however, the combustion efficiency slightly increases from 96.07% to 96.26%. In addition, the high temperature zone near the wall moves to the middle, which protects the combustor liner effectively.

The maximum non-uniformity coefficient is used in this paper to indicate the non-uniformity of outlet, which is defined as the following formula. General requirements: $\theta_t \leq 30\%$,

$$\theta_t = \frac{T_{m,out} - T_{a,out}}{T_{a,out} - T_{a,in}}$$

where *m* means maximum and *a* means average.

Outlet temperature distribution trends consistent, but it is more uniform after the dilution holes because of the increasing combustion and dilution air and the maximum non-uniformity coefficient is 27.93% and 24.67%, respectively. Turbine blades can be better protected in the uniform temperature distribution in the outlet.

Conclusions

Three-dimensional coupled fluid-solid simulations are conducted to investigate the performance of effusion cooling in the real combustion chamber condition. The reliability of the simulation was proved by comparing predicted wall temperature distribution with measurements. The cooling effectiveness of four deflection angle arrangements was investigated and the conclusions are obtained as following.

- The cooling capacity of effusion is better than general film cooling, what's more, the coolant flow rate is reduced by 20%, but the pressure loss is slightly increased.
- Due to the strong injection penetrates and damages the film and local combustion occurs, so the wall temperature increases and the cooling effectiveness decreases behind the primary holes.
- The cooling performance of 60 deg deflection angle is best. The effect of deflection angle is not so significant on the coolant flow rate, but a large negative impact on the pressure loss. The coolant is better attached to the wall downstream when the deflection angle is same as the rotating mainstream.
- Due to the amount of cooling air reduces, the high temperature zone near the wall moves to the middle and the maximum temperature drops about 70 K, the outlet temperature distribution trends more consistent.

Nomenclature

C – specific heat capacity, [$Jkg^{-1}K^{-1}$]
d – effusion hole diameter, [mm]
$\overline{f}$ – mixture fraction
$\overline{f'^2}$ – mixture fraction variance
H – staggered spacing, [mm]
k – turbulent kinetic energy, [m^2s^{-2}]
P – spanwise spacing, [mm]
$p(f)$ – probability density function
PDF – probability density function
S – streamwise spacing, [mm]
T – temperature, [K]

Greek symbols

δ – wall thickness, [mm]
ε – kinetic energy dissipation rate, [m^2s^{-3}]
η – cooling effectiveness
λ – thermal conductivity, [$Wm^{-1}K^{-1}$]

References

[1] Lefebvre, A. H., *et al.*, Gas Turbine Combustion: Alternative Fuels and Emissions, CRC Press, Boca Raton, Fla., USA, 2010
[2] Li, L., *et al*., Combustion and Cooling Performance in an Aero-Engine Annular Combustor, *Applied Thermal Engineering, 26* (2006), 16, pp. 1771-1779
[3] Ali, A. B. S., *et al*., Numerical Investigations of Cooling Holes System Role in the Protection of the Walls of a Gas Turbine Combustion Chamber, *Heat and Mass Transfer, 48* (2012), 5, pp. 779-788

[4] Yu, Z., *et al*., Comparison of a Series of Double Chamber Models with Various Hole Angles for Enhancing Cooling Effectiveness, *International Communications in Heat and Mass Transfer, 44* (2013), May, pp. 38-44
[5] Andrews, G. E., *et al*., Full Coverage Discrete Hole Film Cooling- The Influence of Hole Size, *International Journal of Turbo and Jet-Engines, 2* (1985), 3, pp. 213-225
[6] Andrews, G. E., Hussain, I., Small Diameter Film Cooling Holes: the Influence of Hole Size and Pitch, *International Journal of Turbo and Jet Engines, 5* (1988), 1-4, pp. 61-72
[7] Andrews, G. E., *et al*., Full Coverage Discrete Hole Film Cooling: Cooling Effectiveness, *International Journal of Turbo and Jet-Engines, 2* (1985), 3, pp. 199-212
[8] Lin, Y., *et al*., Investigation of Film Cooling Effectiveness of Full-Coverage Inclined Multihole Walls with Different Hole Arrangements, *Proceedings*, ASME Turbo Expo 2003: Power for Land, Sea, and Air, Atlanta, Geo., USA, 2003, Vol. *5*, pp. 651-660
[9] Zhang, C., *et al*., Cooling Effectiveness of Effusion Walls with Deflection Hole Angles Measured by Infrared Imaging, *Applied Thermal Engineering, 29* (2009), 5, pp. 966-972
[10] Lin, Y., *et al.*, Measured Film Cooling Effectiveness of Three Multihole Patterns, *Journal of Heat Transfer, 128* (2006), 2, pp. 192-197
[11] Scrittore, J. J., *et al.*, Experimental Characterization of Film-Cooling Effectiveness Near Combustor Dilution Holes, *Proceedings*, ASME Turbo Expo 2005: Power for Land, Sea, and Air, Reno, Nevada, USA, 2005, Vol. 3, pp. 1339-1347
[12] Scrittore, J. J., *et al*., Investigation of Velocity Profiles for Effusion Cooling of a Combustor Liner, *Journal of Turbomachinery, 129* (2007), 3, pp. 518-526
[13] Goldstein, R. J., Jin, P., Film Cooling Downstream of a Row of Discrete Holes with Compound Angle, *Journal of Turbomachinery, 123* (2001), 2, pp. 222-230
[14] Ling, J. C. P. W., *et al*., Full Coverage Film Cooling for Combustor Transition Sections, *Proceedings*, ASME Turbo Expo 2002: Power for Land, Sea, and Air, Amsterdam, The Netherlands, 2002, Vol. 3, pp. 1011-1021
[15] Gustafsson, K. M., Johansson, T. G., An Experimental Study of Surface Temperature Distribution on Effusion-Cooled Plates, *Journal of Engineering for Gas Turbines and Power, 123* (2001), 2, pp. 308-316
[16] Yang, C., Zhang, J., Influence of Multi-Hole Arrangement on Cooling Film Development, *Chinese Journal of Aeronautics, 25* (2012), 2, pp. 182-188
[17] Harrington, M. K., *et al*., Full-Coverage Film Cooling with Short Normal Injection Holes, *Journal of Turbomachinery, 123* (2001), 4, pp. 798-805
[18] Tarchi, L., *et al.*, Experimental Investigation on the Effects of a Large Recirculating Area on the Performance of an Effusion Cooled Combustor Liner, *Journal of Engineering for Gas Turbines and Power, 134* (2012), 4, ID 041505
[19] Rohani, B., Saqr, K. M., Effects of Hydrogen Addition on the Structure and Pollutant Emissions of a Turbulent Unconfined Swirling Flame, *International Communications in Heat and Mass Transfer, 39* (2012), 5, pp. 681-688
[20] Zeinivand, H., Bazdidi-Tehrani, F., Influence of Stabilizer Jets on Combustion Characteristics and NOx Emission in a Jet-Stabilized Combustor, *Applied Energy, 92* (2012), Apr., pp. 348-360
[21] Murthy, J. Y., Mathur, S. R., Finite Volume Method for Radiative Heat Transfer Using Unstructured Meshes, *Journal of Thermophysics and Heat Transfer, 12* (1998), 3, pp. 313-321
[22] Dang, X. X., Experimental Investigation and Numerical Simulation of A Gas Turbine Annular Combustor with Dual-Stage Swirler, Ph. D. thesis, Nanjing University of Aeronautics and Astronautics, Nanjing, China, 2009

Paper submitted: January 7, 2014
Paper revised: February 27, 2014
Paper accepted: March 8, 2014